Available online at www.sciencedirect.com

ScienceDirect

Current Opinion in Structural Biology

New insight into cofactor-free oxygenation from combined experimental and computational approaches☆

Soi Bui and Roberto A Steiner

Molecular oxygen (O_2), in spite being a potentially strong oxidant, typically displays very poor reactivity with organic molecules. This is largely due to quantum chemical reasons as O_2 in its ground state is a diradical ($^3O_2$) whilst common organic substrates are in a singlet state. For this reason catalysis involving O_2 as a reactant is typically mediated by enzymes containing redox metal and/or organic co-factors. Cofactor-independent oxygenases (and oxidases) are therefore intriguing enzymes from a fundamental viewpoint. This review looks at recent advances that have been made in understanding of this class of intriguing biocatalysts highlighting the power of an inter-disciplinary approach involving structural biology, spectroscopy and theoretical methods.

Address
Randall Division of Cell and Molecular Biophysics, King's College London, New Hunt's House, Guy's Campus, London SE1 1UL, United Kingdom

Corresponding author: Steiner, Roberto A (roberto.steiner@kcl.ac.uk)

Current Opinion in Structural Biology 2016, **41**:109–118

This review comes from a themed issue on **Catalysis and regulation**

Edited by **David W Christianson** and **Nigel S Scrutton**

For a complete overview see the Issue and the Editorial

Available online 6th July 2016

http://dx.doi.org/10.1016/j.sbi.2016.06.015

Introduction

The incorporation of one or both atoms of molecular oxygen (O_2) into organic substrates is catalyzed by monooxygenases and dioxygenases, respectively. These enzymes, collectively known as oxygenases [1], play a key role in the metabolism of aromatic amino acids [2], fatty acids [3,4], sugars [5], and vitamins [6], as well as in the biosynthesis of collagen [7]. Oxygenation reactions are also used for the degradation of various endogenous and exogenous organic compounds [8], whilst some bacteria employ oxygenases to facilitate the breakdown of molecules that are environmental pollutants [9]. Furthermore, oxygenases can catalyze enantiospecific reactions making them attractive for the production of chiral chemicals, although their industrial application is not without practical problems [10].

From a mechanistic perspective, the task of oxygenases is a difficult one because molecular oxygen in its normal 'resting' state (the form present in the air) is a diradical with a triplet ground-state electronic structure ($^3O_2$) that is not reactive toward the vast majority of singlet-state organic substrates. To deal with this limitation of quantum chemical nature, oxygenases typically rely on transition metals or redox organic cofactors for catalysis [11,12••,13]. A remarkable group of oxygenases, however, can catalyze O_2-incorporation reactions in a cofactor-independent manner [14]. Cofactor-free oxygenases (and oxidases) are therefore intriguing from the viewpoint of fundamental enzymology. In this review we will briefly summarize recent advances in our mechanistic understanding of this fascinating group of enzymes.

Cofactor-free oxygenases

Structural information is available for various cofactor-independent oxygenases including bacterial carbon monoxide-forming 2,4-dioxygenases that degrade quinolones [15••], the vancomycin biosynthetic DpgC dioxygenase [16,17], *Streptomyces coelicolor* ActVA-Orf6 monooxygenase involved in polyketide-tailoring [18], bioluminescent coelenterazine luciferases [19–21], and RhCC from *Rhodococcus jostii* RHA1 whose exact biological role is still unknown [22]. Their three-dimensional structures show that cofactor-independent oxygenation is enabled by a variety of folds and quaternary arrangements (Figure 1). Whilst bacterial carbon monoxide-forming 2,4-dioxygenases (Figure 1a) and *Renilla* coelenterazine luciferase (Figure 1j) are monomeric enzymes belonging to the α/β-hydrolase fold superfamily, DpgC, ActVA-Orf6 and RhCC are assembled into oligomers. Interestingly, *Oplophorus* luciferase (Figure 1k) that catalyzes the same reaction as *Renilla* monooxygenase, relies on a completely different architecture that is similar to those of fatty acid-binding proteins (FABs). The oligomeric ActVA-Orf6 (Figure 1g), that oxidizes 6-deoxydihydrokalafungin to dihydrokalafungin in the biosynthesis of the polyketide antibiotic actinorhodin, is a homodimer in which each

☆ This work was supported by the UK Biotechnology and Biological Sciences Research Council (BBSRC) with a grant (Grant number BB/I020411/1) to RAS.

Figure 1

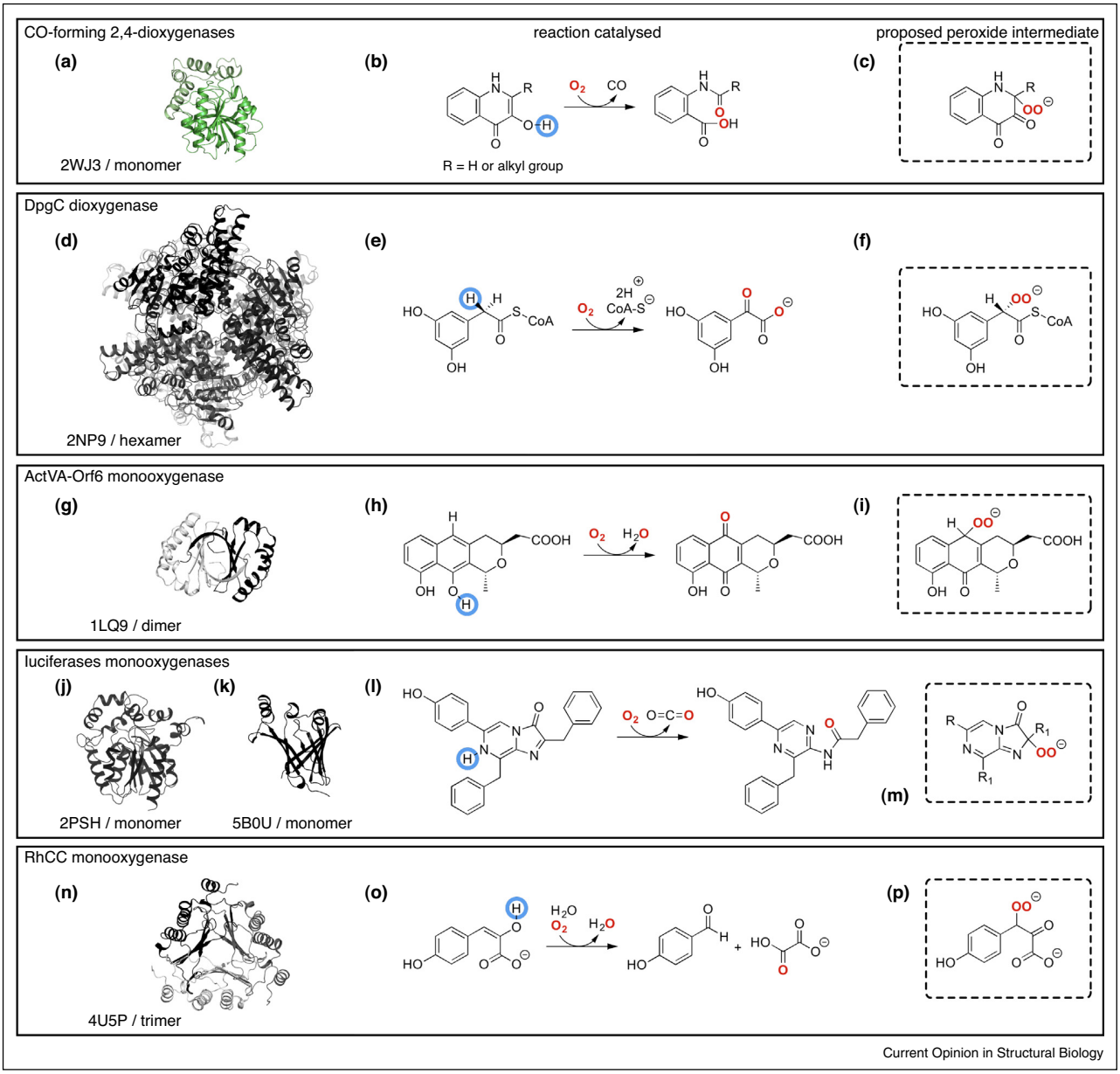

Cofactor-independent oxygenases. Cartoon representations of cofactor-independent oxygenases **(a, d, g, j, k, n)** with schematics of the chemical reaction they catalyze **(b, e, h, l, o)**, and proposed peroxide intermediates **(c, f, i, m, p)**. Structural models are drawn to scale with their PDB code and oligomeric state indicated. Individual chains in the cartoon models are represented in shades of grey, except for (a) that is shown in green. The blue circles in the reaction schemes highlight the protons that are abstracted from the different substrates leading to their activation for reactivity with molecular oxygen (O_2). Oxygen atoms derived from O_2 are shown in red.

protomer displays a ferredoxin-like fold whilst DpgC is a hexamer (Figure 1b) formed by individual chains whose C-terminal region that contains the active site shows homology to the crotonase family of enoyl-CoA isomerase/dehydratases. DpgC is unique as there are no other examples of redox chemistry from this enzyme class. The recently identified RhCC monooxygenase (Figure 1n), is a trimer that belongs to the tautomerase superfamily characterized by a structural β–α–β fold. Like DpgC, RhCC is the first oxygenase identified within this superfamily.

Bacterial cofactor-free dioxygenases involved in the breakdown of *N*-heteroaromatic quinoline derivatives

Our current mechanistic understanding of cofactor-independent oxygenation is largely based on studies

Figure 2

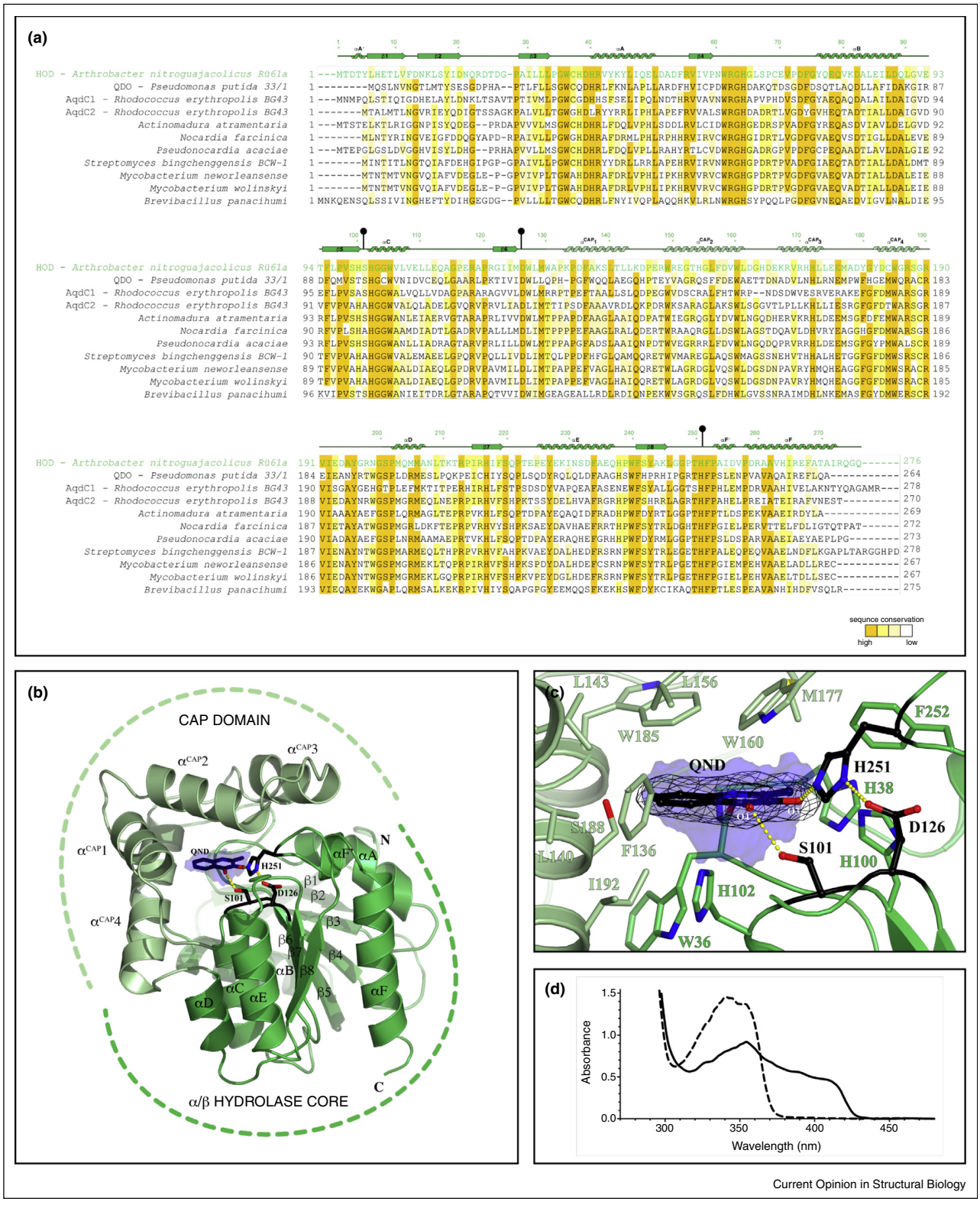

Carbon monoxide (CO)-forming cofactor-independent 2,4-dioxygenases. **(a)** Sequence alignment of various bacterial proteins exhibiting high similarity to *A. nitroguajacolicus* Rü61a 1-*H*-3-hydroxy-4-oxoquinaldine 2,4-dioxygenase (HOD). Residues are highlighted in different shades of

performed on the bacterial carbon monoxide-forming 1-*H*-3-hydroxy-4-oxoquinaldine 2,4-dioxygenase (HOD) from *Arthrobacter nitroguajacolicus* Rü61a. HOD and its homologous 1-*H*-3-hydroxy-4-oxoquinoline 2,4-dioxygenase (QDO) from *Pseudomonas putida* 33/1 were the among first cofactor-free dioxygenases reported in the literature [23]. They are approximately 31-kDa monomeric enzymes that catalyze the O_2-dependent cleavage of the *N*-heteroaromatic ring of quinoline derivatives with concomitant formation of carbon monoxide (Figure 1b). This reaction is chemically identical to that catalyzed by the metal-dependent quercetin dioxygenase [24–26]. However, neither HOD nor QDO are related in sequence to the latter enzyme. HOD and QDO share ~37% sequence identity and constitute a separate family of cofactor-free dioxygenases of the α/β-hydrolase fold superfamily [27]. A BLAST search reveals a number of bacterial proteins with high sequence similarity to HOD/QDO that are likely to be involved in similar breakdown reactions (Figure 2a). Although most of these proteins have not been investigated functionally, a recent report indicates that AqdC1 and AqdC2 from *Rhodococcus erythropolis* BG43 are competent for the degradation of the *Pseudomonas aeruginosa* quorum sensing signal molecule 2-heptyl-3-hydroxy-4(1*H*)-quinolone (PQS, *Pseudomonas* quinolone signal) [28]. Purified recombinant AqdC1 catalyses the O_2-dependent cleavage of PQS to form *N*-octanoylanthranilic acid and CO with an apparent K_m and k_{cat} values of 27 μM and 21 s^{-1}, respectively, thus supporting a 2,4-dioxygenolytic cleavage like that catalyzed by HOD/QDO [28]. Overall, CO-forming bacterial dioxygenases appear to be able to operate on 3-hydroxy-4(1*H*)-quinolones bearing alkyl chains of different length at substrate position 2 (-R in Figure 1b) albeit with different effectiveness.

The structures of both HOD and QDO have been determined by X-ray crystallography [15••] (Figure 2b). As expected on the basis of comparative sequence analysis [29] these dioxygenases belong to the α/β-hydrolase fold superfamily. This is a group of enzymes that rely on a nucleophile-histidine-acidic residue triad to hydrolyze typically C–O, C–N, C–C bonds although a large array of reaction types can be catalyzed by members of this versatile family [30•]. Currently, CO-forming bacterial dioxygenases and the bioluminescent coelenterazine *Renilla* luciferase monooxygenase are the only oxygenases known to employ the α/β-hydrolase scaffold and its catalytic machinery for O_2-dependent catalysis. HOD and QDO, like most enzymes of the α/β-hydrolase fold family, display a two-domain structure constituted by a 'core' domain and a 'cap' domain (Figure 2b). The core domain folds in the canonical α/β hydrolase architecture consisting of a mostly parallel, eight-stranded β sheet surrounded on both sides by α helices (only the second β strand is antiparallel) with the central β sheet featuring a left-handed superhelical 90° twist. The cap domain, formed by four α helices is positioned between β6 and αD. Both domains contribute to delineate the active site cavity. However, only the core domain hosts the nucleophile-histidine-acidic residue catalytic triad, which in the case of HOD is formed by Ser101-His251-Asp126 (Figure 2a,b). A Ser-His-Asp composition is the most common form of the triad [27]. Occasionally, the Ser nucleophile is replaced by a Asp or Cys residue, as in the case of *Renilla* luciferase where the triad is Asp-His-Asp [19].

Substrate activation

A common step in cofactor-independent oxygenation is the initial deprotonation of the bound organic substrate [14,31]. The H^+ ion abstracted in various cofactor-independent-catalyzed reactions is highlighted in Figure 1 (blue circle). The structure of HOD in complex with its natural substrate QND (–R = $–CH_3$ in Figure 1b) obtained under anaerobic conditions reveals that the organic molecule binds in the active site between the core and the cap domains (Figure 2c) with the substrate's O3 atom at H-bond distance to the Nε2 atom of the triad's H251 (2.6 Å) [15••]. This interaction affords the deprotonation of the substrate's hydroxyl group by the His-Asp subset of the triad, essential for substrate activation. Site-directed mutagenesis experiments have shown that replacement of H251 by an alanine (H251A) reduces k_{cat} for QND dioxygenation by several orders of magnitude essentially abolishing catalytic activity [15••,32,33]. Also, replacement of the acidic residue of the triad (D126A) yielded a strongly impaired variant. Consistent with this, density functional theory (DFT) calculations show that the 3OH proton is transferred to His251 in the wild-type system,

(Figure 2 Legend Continued) yellow according to their sequence identity. Secondary structure elements for HOD are also shown for reference with members the catalytic triad marked by an asterisk. Whilst HOD, QDO, AqdC1, AqdC2 are validated CO-forming cofactor-independent 2,4-dioxygenases degrading 3-hydroxy quinoline-derivatives, the other proteins in the alignment likely share the same catalytic activity on the basis of sequence conservation. **(b)** Cartoon representation of the HOD–QND substrate complex with the α/β-hydrolase fold core domain and cap domain shown in dark green and light, respectively. Secondary structure elements are labeled. N and C indicate the N and C termini, respectively. The blue transparent surface highlights the active site cavity where QND is bound. Catalytic triad residues are shown in black as ball-and-stick representation and hydrogen bonds they make are represented by yellow dotted lines. **(c)** Close-up view of the active site in the crystal structure of the anaerobic HOD–QND (enzyme–substrate) complex. $2mF_o - DF_c$ electron density at the 1.30σ level is shown in black for the bound substrate. QND occupies the top portion of the active site cavity (blue) whilst the bottom part is believed to host O_2 during catalysis. Residues lining the active site are in stick representation. **(d)** *In-crystallo* UV–visible spectra of the anaerobic HOD–QND complex (black) and of the aerobic HOD^{H251A}–QND complex (dashed line), recorded at pH 7 and 100 K. The HOD^{H251A} variant is unable to deprotonate the substrates's 3OH group thus preventing substrate activation for O_2 attack.

Figure 3

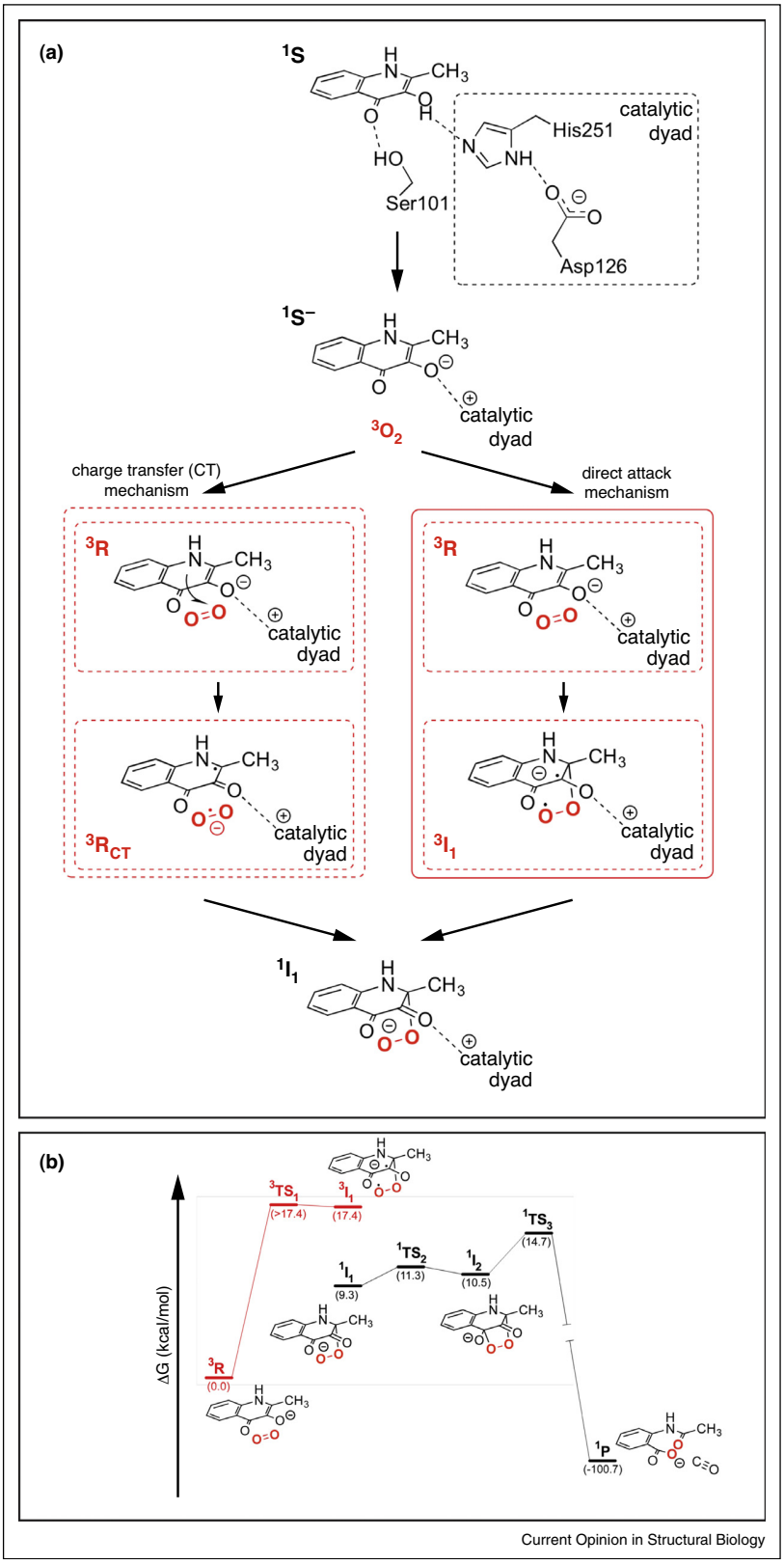
(a)
^{1}S
catalytic dyad
His251
Ser101
Asp126
^{1}S$^-$
catalytic dyad
^{3}O$_2$
charge transfer (CT) mechanism
direct attack mechanism
^{3}R
catalytic dyad
^{3}R$_{CT}$
catalytic dyad
^{3}R
catalytic dyad
^{3}I$_1$
catalytic dyad
^{1}I$_1$
catalytic dyad
(b)
ΔG (kcal/mol)
^{3}R (0.0)
^{3}TS$_1$ (>17.4)
^{3}I$_1$ (17.4)
^{1}I$_1$ (9.3)
^{1}TS$_2$ (11.3)
^{1}I$_2$ (10.5)
^{1}TS$_3$ (14.7)
^{1}P (-100.7)
Current Opinion in Structural Biology

but it remains on the substrate in the HOD^{H251A} and HOD^{D126A} systems [33]. The nucleophile S101 appears to be dispensable for catalysis as S101A replacement only impacted negatively on QND binding as judged by an increase in the K_m constant. The idea of a nucleophile-independent mechanism is further supported by the lack of sequence conservation for this residue whilst the histidine-acidic dyad is strictly invariant (Figure 2a). Kinetic analysis under anoxic transient-state conditions indicates that substrate deprotonation is not rate-limiting as suggested by the 15-fold lower k_{cat} (20 °C) compared with k_H (5 °C) at low pH [33]. Overall, the His-Asp dyad is essential for substrate deprotonation and its consequent activation toward O_2.

How does the activated substrate react with O_2?

Mechanistic concepts borrowed from the field of flavin-dependent oxygenation [34,35] led to the plausible hypothesis that the activated (carb)anion possesses a sufficiently low thermodynamic potential that allows the transfer of an electron to O_2 to generate a substrate radical and superoxide anion [32]. This charge-transfer mechanism is shown for HOD catalysis on the left-hand side of Figure 3a. Following formation of the ($S^{\bullet}$–$O_2^{\bullet-}$) pair ($^3R_{CT}$ in Figure 3a) radical-radical recombination would lead to a C2-(hydro)peroxide ($^1I_1$). To address experimentally the nature of the compounds involved in the reaction with O_2 a recent elegant study used the cyclic hydroxylamine spin probe 1-hydroxy-3-methoxycarbonyl-2,2,5,5-tetramethyl-pyrrolidine (CMH) in the HOD-catalyzed reaction [36••]. Using a HOD variant in which the W160 residue that forms part of the active site cavity (Figure 2c) is substituted by an alanine (HOD^{W160A}) the authors were able to detect significant amounts of CM-nitroxide radical by electron paramagnetic resonance spectroscopy. This variant also released the proposed peroxide intermediate (Figure 1c), which was reduced to the corresponding alcohol and characterized by NMR spectroscopy. These data were interpreted as evidence for two key intermediates in the catalytic mechanism: a substrate radical and a substrate (hydro)peroxide. However, no significant amounts of CM-nitroxide radical were detected when wild-type HOD was used in the reaction. A possible reason for this is that the wild-type protein is able to efficiently shield its active site, whereas the mutant protein may have a more open or more flexible active-site pocket thus allowing access to the CMH probe [36••].

A more recent study put forward an alternative hypothesis for the generation of the peroxide intermediate. On the basis of a combined kinetic, spectroscopic and DFT computational work that takes advantage of available structural information Hernandez-Ortega *et al.* [37••] proposed a novel reaction mechanism that does not involve a formal single electron transfer to dioxygen. The calculations indicate that the $^3R_{CT}$ complex is unable to form spontaneously by electron transfer, and, consequently it is expected that any reactivity of O_2 will come from dioxygen and not from the stabilization of a radical pair. This is proposed to occur with C2 atom of the activated substrate ($^1S^-$) reacting directly with $^3O_2$ to form a C–OO bond as a triplet-state intermediate peroxide ($^3I_1$) (direct attack mechanism in Figure 3a). The latter compound then undergoes an inter-system crossing leading to ($^1I_1$). The reaction energy profile for the direct attack mechanism and subsequent catalytic steps is shown in Figure 3b. Following the formation of ($^1I_1$), attack of the peroxide on the carbonyl function affords the formation of the endoperoxide ($^1I_2$), which then decomposes with the formation of significantly stabilized carbon monoxide and anthranilate derivative products (^1P). Overall, the formation of ($^3I_1$) encounters the highest barrier along the reaction trajectory ($\Delta G^{\ddagger}$ = 17.4 kcal mol^{-1} in a solvent model), and hence is proposed to be the rate limiting step for HOD catalysis. This in agreement with transient-state kinetic studies that show that oxygen-dependent steps are rate-limiting for overall catalysis. Additionally, kinetic and computational analyses show that the W160A substitution decreases the activity dramatically (k_{cat}/K_m is 12,500 ± 600 s^{-1} mM^{-1} and 2.4 ± 0.3 s^{-1} mM^{-1} for wt HOD and HOD^{W160A}, respectively) with energy profiles for the corresponding DFT model showing increased barriers for $^3TS_1$ and $^1TS_3$ [37••]. Thus, the W160A replacement could therefore have an effect on the O_2 activation mechanism.

Peroxide intermediate

The formation of peroxide intermediates is central to the mechanism proposed for essentially all cofactor-independent oxygenases (Figure 1). Yet, their structural elucidation has proven difficult. Urate oxidase (UOX) is a tetrameric cofactor-independent oxidase [14,38] that catalyses the breakdown of urate to 5-hydroxyisourate (5-HIU) with the latter compound further degraded to allantoin (Figure 4a). On the basis of UV–visible spectroscopic evidence, early mechanistic studies suggested that a peroxide adduct (5-PIU) is generated initially by the dioxygenation of the urate dianion (UD)

(Figure 3 Legend) Mechanistic proposals for the CO-forming cofactor-independent 2,4-dioxygenase, HOD. **(a)** Alternative mechanisms for the reaction between the deprotonated QND substrate and O_2. Whilst the charge-transfer mechanism assumes the formation of a substrate–superoxide anion radical pair that leads to the peroxide intermediate, the direct attack mechanism propose the formation of a peroxide diradical that collapses into a lower-energy singlet-state. **(b)** Reaction energy profile of key intermediates and transition states for the reaction catalyzed by HOD following the direct attack mechanism. Solvent corrected Gibbs free energies are given in parenthesis.

Figure 4

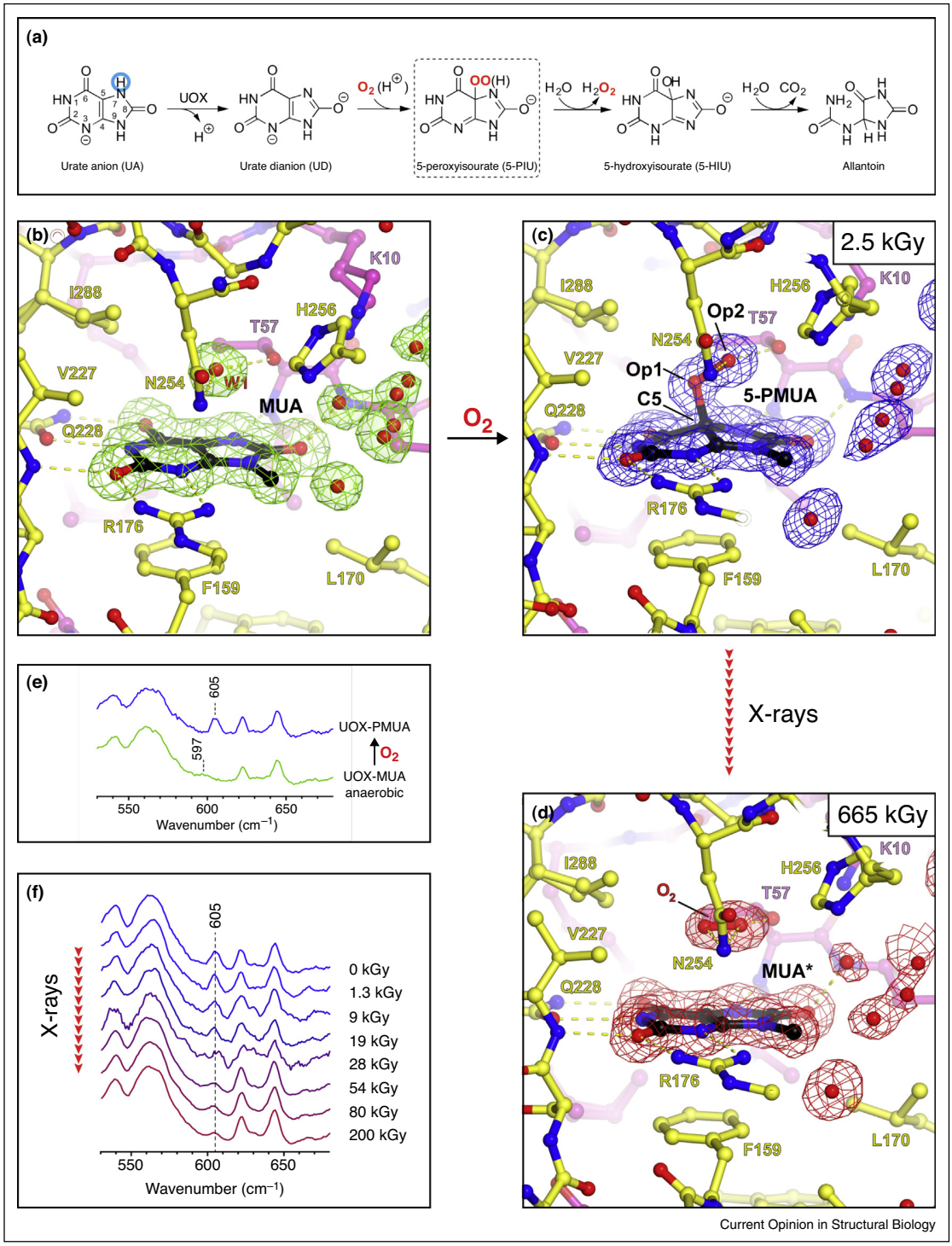

Visualization of the peroxide intermediate formed in the oxygenation step catalyzed by the cofactor-independent oxidase UOX. **(a)** Reaction catalyzed by UOX. The peroxide intermediate has been trapped using the natural substrate UA and also using its 9-methyl derivative (MUA). **(b)** Anaerobic UOX:MUA complex. MUA (like UA) binds at the interface between two subunits (shown in yellow and pink) of the UOX tetramer. Red spheres represent water molecules. H-bonds are shown as broken yellow lines. **(c)** Upon exposure to O_2, the UOX–MUA complex reacts to generate a C5-(hydro)peroxide (5-PMUA). **(d)** The peroxide is specifically radiolyzed at low X-ray dose under cryoconditions generating O_2. **(e)** *In-crystallo* Raman spectroscopy supported by QM/MM calculations show that the band at 605 cm^{-1} is a 5-PMUA 'signature'. **(f)** Online *in-crystallo* Raman spectroscopy reveals the specific dose-dependent decrease of the 605 cm^{-1} 5-PMUA 'signature' band'.

[39]. In subsequent steps H_2O_2 release and H_2O attack at position 5 would form 5-HIU. How UOX exactly contributes to the generation of UD is currently not clear. A mechanism of general base catalysis enabled by a Thr-Lys dyad has been proposed [40] and a neutron diffraction study on the aerobic chloride-inhibited UOX–substrate complex suggested that UD might be generated from the deprotonation of the iminol tautomer of UA [41].

Recently, X-ray crystallography combined with online *in-crystallo* Raman spectroscopy has provided direct evidence for a C5(*S*)-(hydro)peroxide in the initial cofactor-independent dioxygenation stage of the UOX-catalyzed reaction [42••]. Using 9-methyl uric acid (MUA) as substrate, electron density maps at (near)-atomic resolution unambiguously reveal that exposure of the anaerobic UOX–MUA complex (Figure 4b) to O_2 results in MUA conversion into its C5(*S*)-peroxo derivative (5-PMUA) with clear pyramidalization at C5 (Figure 4c). Non-resonant Raman spectra recorded from crystals of anaerobic UOX–MUA and UOX–5PMUA complexes show that the spectral region centered at 600 cm^{-1} reports on changes resulting form the oxygenation reaction (Figure 4e). Upon MUA peroxidation a distinct band develops at 605 cm^{-1} (blue trace) whilst the shoulder at 597 cm^{-1} in the UOX:MUA complex (green) disappears. Quantum mechanics/molecular mechanics (QM/MM) calculations predict a band at 600 cm^{-1} (experimental 605 cm^{-1}) for the 5PMUA (hydro)peroxide resulting form a set of modes involving C5–Op1 bond stretching and C5–Op1–Op2 bending coupled to ring distortions.

Remarkably, the C5–Op1 bond is susceptible to selective radiolysis at very low X-ray doses (Figure 4d,f). Rupture of the C5–Op1 bond is accompanied by the loss of pyramidalization at C5 leading to a planar organic structure while a diatomic molecule 1.2-Å long, consistent with O_2, is liberated and trapped above it (Figure 4d). Dioxygen produced *in situ* adopts a well-defined position with its molecular axis 3.15 Å above the flat organic molecule and both O1 and O2 atoms interacting with N254(Nδ2) at distances of 3.19 Å and 3.09 Å, respectively, whilst the T57(Oγ1) atom is closest to O2 at 2.65 Å. This is consistent with results obtained using room-temperature O_2 pressurization (40 bars) in the presence of the AZA inhibitor [43]. Online Raman analysis shows that peroxide rupture causes the 605 cm^{-1} 'signature' band to selectively decrease in a dose-dependent manner (Figure 4f) consistent with QM/MM calculations that assign this band to the stretching of the C5–Op1 bond.

Conclusions

Interdisciplinary approaches are central to modern enzymology. Structural biology techniques in combination with steady-state and transient-state kinetics, theoretical quantum chemistry calculations, and advanced solution and *in-crystallo* spectroscopic measurements have provided important insight into how cofactor-independent oxygenases work. Although not discussed here, the use of molecular dynamics simulations is also uncovering specific pathways and access points for O_2 in this class of oxygenases that are common to different types of proteins [44•] and often dynamic in nature.

The extensive work carried out on the bacterial cofactor-free 2,4-dioxygeases HOD and studies on various other cofactor-independent oxygenases convincingly suggest that the generation of a substrate (carb)anion is a prerequisite for O_2 reactivity. Thus, these enzymes apparently utilize the intrinsic reactivity of carbanions toward electrophiles as a general catalytic concept [14]. Although the exact mechanism with which O_2 reacts with the activated substrate requires further study, the work of Hernandez-Ortega *et al.* [37••] provides a novel perspective on this reaction by proposing a direct attack to generate a triplet-state peroxide that immediately collapses into a triplet-state. It will be interesting in the future to see whether this novel concept can be generalized to other similar catalytic systems. Finally, using a combination of (online and offline) Raman-assisted X-ray crystallography and theoretical calculations Bui *et al.* [42••] provided unambiguous evidence for a C5-peroxide intermediate in the initial dioxygenation step in UOX cofactor-independent catalysis. Additionally, selective radiolysis afforded exquisite insight into the elusive dioxygen positioning in the ternary E–S–O_2 complex. This experimental information will guide further calculations aimed at addressing O_2 reactivity in this system. The recent advances on cofactor-independent oxygenases discussed here well exemplify the necessity of synergizing experimental and computational approaches in mechanistic enzymology.

Conflict of interest statement

Nothing declared.

References and recommended reading

Papers of particular interest, published within the period of review, have been highlighted as:

- • of special interest
- •• of outstanding interest

1. Yamamoto S: **The 50th anniversary of the discovery of oxygenases**. *IUBMB Life* 2006, **58**:248-250.
2. Fitzpatrick PF: **Mechanism of aromatic amino acid hydroxylation**. *Biochemistry* 2003, **42**:14083-14091.
3. Hamberg M, Ponce de Leon I, Rodriguez MJ, Castresana C: **Alpha-dioxygenases**. *Biochem Biophys Res Commun* 2005, **338**:169-174.
4. Haeggstrom JZ, Funk CD: **Lipoxygenase and leukotriene pathways: biochemistry, biology, and roles in disease**. *Chem Rev* 2011, **111**:5866-5898.

5. Frandsen KE, Simmons TJ, Dupree P, Poulsen JC, Hemsworth GR, Ciano L, Johnston EM, Tovborg M, Johansen KS, von Freiesleben P *et al.*: **The molecular basis of polysaccharide cleavage by lytic polysaccharide monooxygenases**. *Nat Chem Biol* 2016, **12**:298-303.

6. Wyss A: **Carotene oxygenases: a new family of double bond cleavage enzymes**. *J Nutr* 2004, **134**:246S-250S.

7. Myllyharju J: **Prolyl 4-hydroxylases, the key enzymes of collagen biosynthesis**. *Matrix Biol* 2003, **22**:15-24.

8. Meunier B, de Visser SP, Shaik S: **Mechanism of oxidation reactions catalyzed by cytochrome p450 enzymes**. *Chem Rev* 2004, **104**:3947-3980.

9. Furukawa K: **Oxygenases and dehalogenases: molecular approaches to efficient degradation of chlorinated environmental pollutants**. *Biosci Biotechnol Biochem* 2006, **70**:2335-2348.

10. van Beilen JB, Duetz WA, Schmid A, Witholt B: **Practical issues in the application of oxygenases**. *Trends Biotechnol* 2003, **21**:170-177.

11. Pau MY, Lipscomb JD, Solomon EI: **Substrate activation for O_2 reactions by oxidized metal centers in biology**. *Proc Natl Acad Sci U S A* 2007, **104**:18355-18362.

12. •• Kovaleva EG, Lipscomb JD: **Crystal structures of Fe^{2+} dioxygenase superoxo, alkylperoxo, and bound product intermediates**. *Science* 2007, **316**:453-457.

A remarkable example of *in-crystallo* trapping of reaction intermediates in the non-heme Fe^{2+}-dependent homoprotocatechuate 2,3-dioxygenase. Three different intermediates in the O_2 activation and insertion reactions of this extradiol ring-cleaving dioxygenase were visualized including the predicted key substrate–alkylperoxo–Fe^{2+} intermediate.

13. Bugg TDH: **Dioxygenase enzymes: catalytic mechanism and chemical models**. *Tetrahedron* 2003, **59**:7075-7101.

14. Fetzner S, Steiner RA: **Cofactor-independent oxidases and oxygenases**. *Appl Microbiol Biotechnol* 2010, **86**:791-804.

15. •• Steiner RA, Janssen HJ, Roversi P, Oakley AJ, Fetzner S: **Structural basis for cofactor-independent dioxygenation of *N*-heteroaromatic compounds at the alpha/beta-hydrolase fold**. *Proc Natl Acad Sci U S A* 2010, **107**:657-662.

This article describes the crystal structures of alpha/beta-hydrolase fold cofactor-indepedent dioxygenases (HOD and QDO) in their native state as well as the structure of HOD in complex with its natural 1-*H*-3-hydroxy-4-oxoquinaldine substrate, its *N*-acetylanthranilate reaction product, and chloride as dioxygen mimic.

16. Widboom PF, Fielding EN, Liu Y, Bruner SD: **Structural basis for cofactor-independent dioxygenation in vancomycin biosynthesis**. *Nature* 2007, **447**:342-345.

17. Fielding EN, Widboom PF, Bruner SD: **Substrate recognition and catalysis by the cofactor-independent dioxygenase DpgC**. *Biochemistry* 2007, **46**:13994-14000.

18. Sciara G, Kendrew SG, Miele AE, Marsh NG, Federici L, Malatesta F, Schimperna G, Savino C, Vallone B: **The structure of ActVA-Orf6, a novel type of monooxygenase involved in actinorhodin biosynthesis**. *EMBO J* 2003, **22**:205-215.

19. Loening AM, Fenn TD, Gambhir SS: **Crystal structures of the luciferase and green fluorescent protein from *Renilla reniformis***. *J Mol Biol* 2007, **374**:1017-1028.

20. Schultz LW, Liu L, Cegielski M, Hastings JW: **Crystal structure of a pH-regulated luciferase catalyzing the bioluminescent oxidation of an open tetrapyrrole**. *Proc Natl Acad Sci U S A* 2005, **102**:1378-1383.

21. Tomabechi Y, Hosoya T, Ehara H, Sekine S, Shirouzu M, Inouye S: **Crystal structure of nanoKAZ: the mutated 19 kDa component of *Oplophorus* luciferase catalyzing the bioluminescent reaction with coelenterazine**. *Biochem Biophys Res Commun* 2016, **470**:88-93.

22. Baas BJ, Poddar H, Geertsema EM, Rozeboom HJ, de Vries MP, Permentier HP, Thunnissen AM, Poelarends GJ: **Functional and structural characterization of an unusual cofactor-independent oxygenase**. *Biochemistry* 2015, **54**:1219-1232.

23. Bauer I, Max N, Fetzner S, Lingens F: **2,4-Dioxygenases catalyzing N-heterocyclic-ring cleavage and formation of carbon monoxide. Purification and some properties of 1*H*-3-hydroxy-4-oxoquinaldine 2,4-dioxygenase from *Arthrobacter* sp. Ru61a and comparison with 1H-3-hydroxy-4-oxoquinoline 2,4-dioxygenase from *Pseudomonas putida* 33/1**. *Eur J Biochem* 1996, **240**:576-583.

24. Jeoung JH, Nianios D, Fetzner S, Dobbek H: **Quercetin 2,4-dioxygenase activates dioxygen in a side-on O_2–Ni complex**. *Angew Chem Int Ed Engl* 2016, **55**:3281-3284.

25. Gopal B, Madan LL, Betz SF, Kossiakoff AA: **The crystal structure of a quercetin 2,3-dioxygenase from *Bacillus subtilis* suggests modulation of enzyme activity by a change in the metal ion at the active site(s)**. *Biochemistry* 2005, **44**:193-201.

26. Steiner RA, Kalk KH, Dijkstra BW: **Crystal structures of anaerobic enzyme·substrate complexes provide insight into the reaction mechanism of the copper-dependent quercetin 2,3-dioxygenase**. *Proc Natl Acad Sci U S A* 2002, **99**:16625-16630.

27. Nardini M, Dijkstra BW: **Alpha/beta hydrolase fold enzymes: the family keeps growing**. *Curr Opin Struct Biol* 1999, **9**:732-737.

28. Muller C, Birmes FS, Ruckert C, Kalinowski J, Fetzner S: ***Rhodococcus erythropolis* BG43 genes mediating *Pseudomonas aeruginosa* quinolone signal degradation and virulence factor attenuation**. *Appl Environ Microbiol* 2015, **81**:7720-7729.

29. Fischer F, Künne S, Fetzner S: **Bacterial 2,4-dioxygenases: new members of the alpha/beta hydrolase-fold superfamily of enzymes functionally related to serine hydrolases**. *J Bacteriol* 1999, **181**:5725-5733.

30. • Rauwerdink A, Kazlauskas RJ: **How the same core catalytic machinery catalyzes 17 different reactions: the serine–histidine–aspartate catalytic triad of α/β-hydrolase fold enzymes**. *ACS Catal* 2015, **5**:6153-6176.

Up-to-date review highlighting the versatility of the α/β-hydrolase fold equipped with the Ser-His-Asp catalytic triad.

31. Fetzner S: **Oxygenases without requirement for cofactors or metal ions**. *Appl Microbiol Biotechnol* 2002, **60**:243-257.

32. Frerichs-Deeken U, Ranguelova K, Kappl R, Huttermann J, Fetzner S: **Dioxygenases without requirement for cofactors and their chemical model reaction: compulsory order ternary complex mechanism of 1*H*-3-hydroxy-4-oxoquinaldine 2,4-dioxygenase involving general base catalysis by histidine 251 and single-electron oxidation of the substrate dianion**. *Biochemistry* 2004, **43**:14485-14499.

33. Hernandez-Ortega A, Quesne MG, Bui S, Heuts DP, Steiner RA, Heyes DJ, de Visser SP, Scrutton NS: **Origin of the proton-transfer step in the cofactor-free (1*H*)-3-hydroxy-4-oxoquinaldine 2,4-dioxygenase: effect of the basicity of an active site His residue**. *J Biol Chem* 2014, **289**:8620-8632.

34. Massey V: **Activation of molecular oxygen by flavins and flavoproteins**. *J Biol Chem* 1994, **269**:22459-22462.

35. Mattevi A: **To be or not to be an oxidase: challenging the oxygen reactivity of flavoenzymes**. *Trends Biochem Sci* 2006, **31**:276-283.

36. •• Thierbach S, Bui N, Zapp J, Chhabra SR, Kappl R, Fetzner S: **Substrate-assisted O_2 activation in a cofactor-independent dioxygenase**. *Chem Biol* 2014, **21**:217-225.

Elegant work that uses a multi-disciplinary approach supporting a mechanism of charge transfer for the reaction of O_2 with the activated substrate in cofactor-free 2,4-dioxygenases. This study also presents evidence for a peroxide intermediate during catalysis.

37. •• Hernandez-Ortega A, Quesne MG, Bui S, Heyes DJ, Steiner RA, Scrutton NS, de Visser SP: **Catalytic mechanism of cofactor-free dioxygenases and how they circumvent spin-forbidden oxygenation of their substrates**. *J Am Chem Soc* 2015, **137**:7474-7487.

This study combines kinetics, spectroscopic and computational approaches. It proposes that in cofactor-free 2,4-dioxygenases the reaction is initiated by triplet dioxygen and its binding to deprotonated substrate and only thereafter a spin state crossing to the singlet spin state occurs.

38. Colloc'h N, el Hajji M, Bachet B, L'Hermite G, Schiltz M, Prange T, Castro B, Mornon JP: **Crystal structure of the protein drug urate oxidase–inhibitor complex at 2.05 Å resolution**. *Nat Struct Biol* 1997, **4**:947-952.

39. Kahn K, Tipton PA: **Spectroscopic characterization of intermediates in the urate oxidase reaction**. *Biochemistry* 1998, **37**:11651-11659.

40. Imhoff RD, Power NP, Borrok MJ, Tipton PA: **General base catalysis in the urate oxidase reaction: evidence for a novel Thr-Lys catalytic diad**. *Biochemistry* 2003, **42**:4094-4100.

41. Oksanen E, Blakeley MP, El-Hajji M, Ryde U, Budayova-Spano M: **The neutron structure of urate oxidase resolves a long-standing mechanistic conundrum and reveals unexpected changes in protonation**. *PLOS ONE* 2014, **9**:e86651.

42. •• Bui S, von Stetten D, Jambrina PG, Prange T, Colloc'h N, de Sanctis D, Royant A, Rosta E, Steiner RA: **Direct evidence for a peroxide intermediate and a reactive enzyme–substrate–dioxygen configuration in a cofactor-free oxidase**. *Angew Chem Int Ed Engl* 2014, **53**:13710-13714.

In this work near-atomic resolution crystallography supported by *in-crystallo* Raman spectroscopy and QM/MM calculations show unambiguously that the archetypical cofactor-free uricase catalyzes the first oxygenation step in the degradation of urate via a C5(*S*)-(hydro)peroxide intermediate. Additionally, low X-ray doses break specifically the intermediate C5–OO(H) bond at 100 K, thus releasing O_2 *in situ*, which is trapped above the substrate radical providing a snapshot of the E–S–O_2 complex.

43. Colloc'h N, Prange T: **Functional relevance of the internal hydrophobic cavity of urate oxidase**. *FEBS Lett* 2014, **588**:1715-1719.

44. • Di Russo NV, Condurso HL, Li K, Bruner SD, Roitberg AE: **Oxygen diffusion pathways in a cofactor-independent dioxygenase**. *Chem Sci* 2015, **6**:6341-6348.

This study uses a combined molecular dynamics and experimental approach to look at O_2 access pathways in the cofactor-independed dioxygenase DpgC. Multiple access channels are available, and the architecture of the pathway network can provide regioselectivity and stereoselectivity. Overall, it appears that there are common themes in O_2 access that are conserved among very different types of proteins.